2006

Aggregation of Robust Regularization with Dynamic Filtration for Enhanced Radar Imaging

Shkvarko, Yuriy; Villalón-Turrubiates, Iván E.; Leyva-Montiel, José L.

Yuriy V. Shkvarko, Iván E. Villalón-Turrubiates y José L. Leyva-Montiel (2006). “Aggregation of Robust Regularization with Dynamic Filtration for Enhanced Radar Imaging”, Journal of Applied Radioelectronics, 5(3), pp.316-325.

AGGREGATION OF ROBUST REGULARIZATION WITH DYNAMIC FILTRATION FOR ENHANCED RADAR IMAGING

Yuriy V. SHKVARKO, Ivan E. VILLALON-TURRUBIATES and Jose L. LEYVA-MONTIEL

The paper suggest a novel approach to the problem of high-resolution array radar/SAR imaging as an ill-conditioned inverse spatial spectrum pattern (SSP) estimation problem with model uncertainties. We explain the theory recently developed by the authors of this presentation that addresses a new fused Bayesian-regularization paradigm for radar/SAR image formation/reconstruction. We show how this theory leads to new adaptive and robustified computational methods that enable one to derive efficient and consistent estimates of the SSP via unifying the Bayesian minimum risk estimation strategy with the ME randomized a priori image model and other projection-type regularization constraints imposed on the solution. We detail such fused Bayesian-regularization (FBR) paradigm and analyze some efficient numerical schemes for computational implementation of the relevant FBR-based methods. Also, we present the results of extended simulation study of the family of the radar image (RI) formation algorithms that employ the proposed FBR paradigm for high-resolution reconstruction of the SSP of the wavefield sources distributed in the remotely sensed environment. The last issue that we address as a perspective innovation is a paradigm of incorporating the concept of dynamic computing into the FBR-based technique to enable the latter to reconstruct the desired environmental remote sensing signatures (RSS) extracted from the enhanced imagery taking into account their dynamical behaviour. This provides a background for understanding the future trends in development of intelligent dynamic RS imaging and resource management techniques. The advantages of the well designed RI experiments (that employ the FBR-based methods) over the cases of poorer designed experiments (that employ the matched spatial filtering as well as the constrained least squares estimators) are investigated trough the simulation study.

1. INTRODUCTION

The goal of this presentation is to address and discuss a new approach to high-resolution radar/SAR imaging as an ill-conditioned inverse problem of estimating the spatial spectrum pattern (SSP) of the wavefield sources scattered from the probing surface (referred to as the radar/SAR image). We explain the theory recently developed by the authors of this presentation [4] – [13] that addresses a new fused Bayesian-regularization (FBR) paradigm for enhanced radar/SAR image formation/ reconstruction. We show how to derive the efficient and consistent estimates of the SSP via unifying the Bayesian minimum risk estimation strategy [2] with the ME randomized a priori image model and other projection-type regularization constraints imposed on the solution [3], [5]. The principal innovative contribution of this study may be briefly sumarized as follows:

1. Development of the grounded statistical randomized model of the radar/SAR imaging experiment via combining the maximum entropy (ME) principle of information theory and regularization concept for alleviating the ill-poseness of the nonlinear inverse problem of estimating the SSP of the wavefield scattered from the probing surface via processing the finite number of the sampled recordings of the radar/SAR data signals.
2. Design of a technique for *optimal* solution of such nonlinear SSP estimation inverse problem in a concise algorithmic form, *optimal* being considered in the fused Bayesian-regularization setting.

Having addressed the FBR method, we then discuss some new efficient numerical schemes for implementing the FBR-related techniques that are indicative of the computational advances in unifying the Bayesian and regularization paradigms for enhanced radar/SAR imaging. The FBR methodology is based on the aggregation of the Bayesian minimum risk statistical optimal estimation strategy [1], [2], [7] with the descriptive weighted constrained least squares optimization technique [1] that involves the non trivial a priori information on the desired properties of the SSP to be reconstructed from the actually measured data signals. Those may employ the specific metrics properties of the image space, boundary value conditions, calibration constraints, bench marks on the image scene [1], [3], [8], etc. In the applications related to passive and active radar remote sensing (RS), the unified FBR method was conceptually developed in our previous studies [4] – [13].

Also, we are going to present the results of extended simulation studies of the family of the FBR-based SSP estimation algorithms tested in the framework of the RI formation/reconstruction experiment. The use of MATLAB as simulation tools provided the computational efficiency and flexibility in performing all simulation experiments.

The family of the FBR-based SSP estimation (RI reconstruction) techniques that we investigate in this study

trough computer simulations comprises the following basic estimators:

1. The simplest matched spatial filtering (MSF) algorithm for RI formation.
2. The descriptive constrained least squares (CLS) RI reconstruction algorithm.
3. The modified descriptive weighted constrained least squares (WCLS) algorithm.
4. The adaptive spatial filtering (ASF) algorithm.
5. The general FBR estimator for the SSP and its robustified version (RFBR).
6. The aggregated FBR-MVDR algorithm for reconstructive RS imagery.

The aim of the simulation experiment was to investigate the performances of these above listed six FBR-based SSP estimators.

2. ENHANCED RADAR IMAGING - A REVIEW

The SSP estimation problem is a statistical ill-conditioned nonlinear inverse problem [4], [5]. Because of the stochastic nature and nonlinearity, *no unique regular* method exists for reconstructing the SSP from the finite-dimensional measurement data in an analytic closed form. Hence, the particular solution strategy to be developed and applied must unify the practical data observation method with some form of statistical regularization that incorporates the a priori model knowledge about the SSP to alleviate the problem ill-poseness.

The classical imaging with radar or SAR implies application of the method called "matched spatial filtering" (MSF) that originates from the celebrated maximum likelihood (ML) estimation strategy [2] to process the recorded data signals. In the statistical terms [2], [4], such a method implies application of the adjoint SFO to the recorded data, computation of the squared norm of a filter outputs and their averaging over the actually recorded samples (the so-called *snapshots* [2]) of the independent data observations.

As it was analyzed in many works, e.g. [1] – [13], the MSF method does not exploit all the "degrees of freedom" of the problem at hand, thus manifests low spatial resolution performances. The recent approaches to high-resolution enhanced radar/SAR imaging are based on treatment the problem at hand as an ill-posed nonlinear inverse problem with model uncertainties [4] – [13]. The principal idea is to fuse the statistical Bayesian minimum risk and descriptive regularization-based paradigms to resolve the SSP estimation inverse problem with minimum risk (i.e. maximum spatial resolution) subject to non-trivial ME and other projection-type constraints imposed on the solution (i.e. incorporate the a priori model information with minimum subjective decision making).

3. PROBLEM MODEL

In radar imaging [1], [3] the backscattered field of the remotely sensed/probing surface $X \ni \mathbf{x}$ is modeled by imposing its time invariant complex scattering function $e(\mathbf{x})$ over the object scene $X \ni \mathbf{x}$. The measurement data wavefield $u(\mathbf{y}) = s(\mathbf{y}) + n(\mathbf{y})$ consists of the echo signals s and additive noise n, and is available for observations and recordings within the prescribed time-space observation domain $Y = T \times P$, where $\mathbf{y} = (t, \mathbf{p})^{\mathrm{T}}$ defines the time-space points in Y. The model of the observation wavefield u is defined by specifying the stochastic equation of observation of an operator form [4]: $u = Se + n$; $e \in \mathrm{E}$; $u, n \in \mathrm{U}$; $S: \mathrm{E} \to \mathrm{U}$, in the Gilbert signal spaces E and U with the metric structures induced by the inner products,

$$[u_1, u_2]_{\mathrm{U}} = \int_Y u_1(\mathbf{y}) u_2^*(\mathbf{y}) d\mathbf{y} ,$$

and

$$[e_1, e_2]_{\mathrm{E}} = \int_X e_1(\mathbf{x}) e_2^*(\mathbf{x}) d\mathbf{x} ,$$

respectively. All the fields e, n, u are assumed to be zero-mean complex valued Gaussian random fields. Next, we assume an incoherent nature of the backscattered field $e(\mathbf{x})$. This is naturally inherent to the radar imaging experiments [1], [3] and leads to the δ-form of the object field correlation function, $R_e(\mathbf{x}_1,\mathbf{x}_2) = B(\mathbf{x}_1)\delta(\mathbf{x}_1 - \mathbf{x}_2)$, where $e(\mathbf{x})$ and $B(\mathbf{x}) = \langle |e(\mathbf{x})|^2 \rangle$ are referred to as a random complex scattering function of the probing surface and its average power scattering function or spatial spectrum pattern (SSP), respectively.

The problem of enhanced radar/SAR imaging is to develop a data processing method for performing the high efficient estimation of the SSP $B(\mathbf{x})$ as a function of the probing surface $X \ni \mathbf{x}$ by processing the available data wavefield recordings $u(\mathbf{y})$ measured over the AA/SA trajectory $Y \ni \mathbf{y}$. Such the estimate $\hat{B}(\mathbf{x})$ of the SSP $B(\mathbf{x})$ is referred to as the desired enhanced radar/SAR image of the probing surface [4].

In the conventional vector form, the estimate $\hat{\mathbf{B}}$ of the vectorized SSP model defines the desired discrete-form image of the remotely sensed scene in the adopted pixel image format [3]. The vector-form data is modeled by the equation of observation

$$\mathbf{U} = \mathbf{SE} + \mathbf{N} \qquad (1)$$

where $\mathbf{E}$ is the original K-D vector of the discrete-form approximation of the random complex object scattering function (SF) $e(\mathbf{x})$, the K-by-M matrix $\mathbf{S}$ is referred to as the linear signal formation operator (SFO) and $\mathbf{N}$ represents the observation noise vector (in this study, we accept the robust white noise model, i.e. $\mathbf{R}_{\mathbf{N}}^{-1} = (1/N_0)\mathbf{I}$, with the noise intensity N_0 pre-estimated by some means [4]. The vector-form approximation of the SSP relates to the original complex random SF vector $\mathbf{E}$ as [4], [7], $\mathbf{B} = \{\langle \mathbf{E}\mathbf{E}^{+} \rangle\}_{\mathrm{diag}}$.

4. FBR METHOD – AN OVERVIEW

The general FBR method for enhanced AA/SAR imaging developed in [4], [5], [8] comprise two following estimators.

4.1 Iterative Adaptive Spatial Filtering (ASF) Estimator of the SSP

Defined as follows [4]

$$\hat{\mathbf{B}}_{ASF} \rightarrow \hat{\mathbf{B}}^{(i+1)} = \hat{\mathbf{B}}^{(i)} + \zeta(\mathbf{W}[\mathbf{V}(\hat{\mathbf{B}}^{(i)}) - \mathbf{Z}_{\Sigma}(\hat{\mathbf{B}}^{(i)})] - (\hat{\mathbf{B}}^{(i)} - \mathbf{B}_{\mathrm{pr}})) \quad (2)$$

with the initial iteration $\hat{\mathbf{B}}^{(0)}$ taken as some prior model of the SSP, e.g. $\hat{\mathbf{B}}^{(0)} = \mathbf{B}_{\mathrm{pr}}$, where superscript $i = 0, 1, 2, \ldots$ represents the iteration step number, ζ is the relaxation parameter, and

$$\mathbf{Z}_{\Sigma}(\hat{\mathbf{B}}^{(i)}) = \mathbf{T}(\hat{\mathbf{B}}^{(i)})\mathbf{B}_0 + \mathbf{Z}(\hat{\mathbf{B}}^{(i)}) \quad (3)$$

defines the total shift to the sufficient statistics (SS) at the ith iteration. In (2),

$$\mathbf{V} = \{\mathbf{F}\mathbf{U}\mathbf{U}^{+}\mathbf{F}^{+})\}_{\mathrm{diag}} \quad (4)$$

represents the vector of smooth SS that is formed applying the SS formation operator

$$\mathbf{F} = \mathbf{F}(\mathbf{B}) = \mathbf{D}(\mathbf{B})\,(\mathbf{I} + \mathbf{S}^{+}\mathbf{R}_{\mathbf{N}}^{-1}\mathbf{S}\mathbf{D}(\mathbf{B}))^{-1}\mathbf{S}^{+}\mathbf{R}_{\mathbf{N}}^{-1} \quad (5)$$

to the trajectory data $\mathbf{U}$. Also in (3),

$$\mathbf{Z} = \mathbf{Z}(\mathbf{B}) = \{\mathbf{F}\mathbf{R}_{\mathbf{N}}\mathbf{F}^{+}\}_{\mathrm{diag}} \quad (6)$$

is the bias vector, $\mathbf{T} = \mathrm{diag}\{\{\mathbf{S}^{+}\mathbf{F}^{+}\mathbf{F}\mathbf{S}\}_{\mathrm{diag}}\}$, and

$$\mathbf{W} = \mathbf{P}\boldsymbol{\Omega} \quad (7)$$

defines the window operator: a composition of the smoothing filter $\boldsymbol{\Omega}$ and the projector $\mathbf{P}$ onto the proper solution space, which must be designed to aggregate the corresponding metrics and projection constraints imposed on the solution (see [4], [5], [9] for details).

4.2 Robust Spatial Filtering (RSF) estimator

$$\hat{\mathbf{B}}_{RSF} = \boldsymbol{\Omega}\mathbf{V} \quad (8)$$

That relates to (2) as its robustified version for the case of trivial priors, $\mathbf{B}_{\mathrm{pr}} = \mathbf{0}$, $\mathbf{P} = \mathbf{I}$, and solution independent approximation

$$\mathbf{F} = (\mathbf{I} + \rho^{-1}\mathbf{S}^{+}\mathbf{S})^{-1}\mathbf{S}^{+} \quad (9)$$

of the SS formation operator with the inverse ρ^{-1} of the SNR $\rho = \beta/N_0$ as a regularization parameter, where β represents the image average gray level preestimated by some means [4].

4.3 Matched spatial filtering (MSF) estimator

This represents the further simplification of the RSF [1]. Adopting the trivial a priori model information ($\mathbf{P} = \mathbf{I}$ and $\mathbf{B}_{\mathrm{pr}} = \mathbf{0}$) and roughly approximating the SS formation operator $\mathbf{F}$ by the adjoint SFO, i.e. $\mathbf{F} \approx \gamma_0\mathbf{S}^{+}$ (where the normalizing constant γ_0 provides balance of the operator norms $\gamma_0^2\,\mathrm{tr}\{\mathbf{S}^{+}\mathbf{S}\mathbf{S}^{+}\mathbf{S}\}=\mathrm{tr}\{\mathbf{F}\mathbf{S}\mathbf{S}^{+}\mathbf{F}^{+}\}$), the (8) can be simplified to the classical *MSF* estimator

$$\hat{\mathbf{B}}_{MSF} = \boldsymbol{\Omega}\mathbf{H}, \quad (10)$$

where the rough SS, $\mathbf{H} = \gamma_0^2\,\{\mathbf{S}^{+}\mathbf{U}\mathbf{U}^{+}\mathbf{S}\}_{\mathrm{diag}}$, is now formed applying the adjoint operator $\mathbf{S}^{+}$, and the windowing of the rough SS $\mathbf{H}$ is performed applying the smoothing filter $\boldsymbol{\Omega}$ that was constructed numerically in [4], [5], the *MSF* algorithm (10) coincides with the conventional aperture synthesis procedure [2], [3] with the matched filtering of the array/trajectory signal as the data processing method, whereas, the *RSF* and *ASF* estimators (8) and (2), respectively, may be referred to as the enhanced imaging algorithms that provide the image improvement/ reconstruction with respect to that formed using the conventional *MSF* method.

5. SUMMARY OF THE FBR-BASED SSP ESTIMATORS

The family of the SSP estimation (reconstruction) algorithms that employ the FBR technique originally proposed in [1], [4], and developed further in [9] comprises the following estimators.

5.1 General FBR estimator of the SSP

Defined as follows,

$$\begin{aligned}\hat{\mathbf{B}}_{FBR} &= \{\mathbf{F}\mathbf{Y}\mathbf{F}^{+}\}_{\mathrm{diag}} \\ &= \mathbf{K}_{\mathbf{A},\alpha}\mathbf{S}^{+}\mathbf{R}_{\mathbf{N}}^{-1}\mathbf{Y}\,\mathbf{R}_{\mathbf{N}}^{-1}\mathbf{S}\mathbf{K}_{\mathbf{A},\alpha}\}_{\mathrm{diag}} \\ &= \{\mathbf{K}_{\mathbf{A},\alpha}\underset{j\in J}{\mathrm{aver}}\,\{\mathbf{Q}_{(j)}\mathbf{Q}^{+}_{(j)}\}\mathbf{K}_{\mathbf{A},\alpha}\}_{\mathrm{diag}},\end{aligned} \quad (11)$$

where

$$\mathbf{F} = \mathbf{K}_{\mathbf{A},\alpha}\mathbf{S}^{+}\mathbf{R}_{\mathbf{N}}^{-1}$$

this is the FBR-optimized Image Formation Operator (IFO) in which

$$\mathbf{K}_{\mathbf{A},\alpha} = (\mathbf{S}^{+}\mathbf{R}_{\mathbf{N}}^{-1}\mathbf{S} + \alpha\mathbf{A}^{-1})^{-1}$$

represents the so-called reconstructive operator where α is the regularization parameter and $\mathbf{A}$ is the weight matrix. Parameter α and matrix $\mathbf{A}$ comprise the regularization degrees of freedom of the general FBR estimator (11),

$$\hat{\mathbf{B}}_{FBR} = \{\hat{\mathbf{D}}\}_{\mathrm{diag}} \quad (12)$$

defines the estimate of the K-D SSP vector $\mathbf{B}=\{<\mathbf{E}\mathbf{E}^{+}>\}_{\mathrm{diag}}$ and

$$\mathbf{Y} = \underset{j\in J}{\mathrm{aver}}\,\{\mathbf{U}_{(j)}\mathbf{U}^{+}_{(j)}\} = \hat{\mathbf{R}}_{\mathbf{U}} \quad (13)$$

is the estimate of the M-by-M data correlation matrix. Here, $\mathbf{U}_{(j)}$ represents the jth realization of the M-D complex measurement data vector specified by (1). Also, in (11),

$$\mathbf{Q}_{(j)} = \{\mathbf{S}^{+}\mathbf{R}_{\mathbf{N}}^{-1}\mathbf{U}_{(j)}\} \quad (14)$$

defines an output of the matched spatial filtering (MSF) algorithm with noise whitening. The robustified version (*RFBR*) of the general FBR estimator (11) is constructed as an iterative scheme for solving (1) with respect to $\mathbf{B}$ with optimally adjusted $\mathbf{A} = \hat{\mathbf{D}}^{-1}$ [4]. While performing the

iterations, $\mathbf{A}^{(i)}$ at the current iteration i = 0, 1, … is approximated by the estimate $\hat{\mathbf{D}}^{-1}$ obtained at the previous iteration with the initial guess $\hat{\mathbf{D}}_0 = B_0\mathbf{I}$, i.e. approximated by the average gray level B_0 in all image pixels [6], [10].

5.2 Descriptive Constrained Least Squares (CLS) estimator

Is constructed as modification of (11) for the following re-adjustments: $\mathbf{A} = \mathbf{I}$ and $\alpha = N_0/B_0$, i.e. the inverse of the signal-to-noise ratio (SNR), where B_0 is the prior average gray level of the SSP. In that case, the IFO $\mathbf{F}$ is recognized to be the Tikhonov's CLS spatial filter

$$\mathbf{F}_{CLS} = (\mathbf{S}^{+}\mathbf{S} + \alpha\,\mathbf{I})^{-1}\mathbf{S}^{+}. \qquad (15)$$

5.3 Descriptive Weighted Constrained Least Squares (WCLS) estimator

Is constructed as a *modified* version of (15) for the following re-adjustments of the degrees of freedom: $\mathbf{A}=\mathbf{M_B}$; $\alpha=N_0/B_0$,

$$\mathbf{F}_{WCLS} = (\mathbf{S}^{+}\mathbf{S} + \alpha\,\mathbf{M_B})^{-1}\mathbf{S}^{+} \qquad (16)$$

where $\mathbf{M_B}$ represents the Tikhonov's stabilizer of the second order constructed numerically in [4].

5.4 Matched spatial filtering (MSF)

SSP estimation algorithm is given by the simplified version of (15) for an assumption, $\alpha >> \|\mathbf{S}^{+}\mathbf{S}\|$, which yields

$$\mathbf{F}_{MSF} \approx const \cdot \mathbf{S}^{+}, \qquad (17)$$

hence, the rough MSF image is formed applying the adjoint SFO $\mathbf{S}^{+}$.

5.5 Adaptive spatial filtering (ASF) algorithm

Is constructed as modification of (11) for the case of an arbitrary zero-mean noise with the correlation matrix $\mathbf{R_N}$, the equal importance of the systematic and noise error measures [1], i.e. α = 1, and the solution dependent weight matrix $\mathbf{A} = \hat{\mathbf{D}}^{-1}$. In this case, the IFO is recognized to be the adaptive spatial filter

$$\mathbf{F}_{ASF} = (\mathbf{S}^{+}\mathbf{R}_{\mathbf{N}}^{-1}\mathbf{S} + \hat{\mathbf{D}}^{-1})^{-1}\mathbf{S}^{+}\mathbf{R}_{\mathbf{N}}^{-1}. \qquad (18)$$

5.6 Aggregated FBR-MVDR estimator

Constructed as $\hat{\mathbf{B}}_{FBR-MVDR} = \{\mathbf{F}_{FBR\text{-}MVDR}\mathbf{Y}\mathbf{F}^{+}_{FBR\text{-}MVDR}\}_{\text{diag}}$ with the IFO given by [4]

$$\mathbf{F}_{FBR\text{-}MVDR} = (\mathbf{S}^{+}\mathbf{S} + N_0\,\hat{\mathbf{D}}^{-1})^{-1}\mathbf{S}^{+}. \qquad (19)$$

Such $\mathbf{F}_{FBR\text{-}MVDR}$ is recognized to be the IFO that minimizes the Bayesian risk [4], [11] of estimates $\hat{\mathbf{B}}$.

It is obvious that the MVDR, ASF and RFBR estimators may be considered as particular cases of the uniform FBR image formation algorithm (11) under the model assumptions specified above.

Hence, by controlling the regularization degrees of freedom, $\mathbf{A}$, α, one can proceed from the general FBR estimator (11) to the variety of different image formation algorithms, from the simplest matched spatial filtering to the adaptive beamforming techniques.

6. TOWARDS DYNAMICAL COMPUTING FOR RECONSTRUCTION

6.1 RSS linear dynamic model

The crucial issue in application of the modern dynamic filter theory [8], [9], [13] to the problem of reconstruction of the desired RRS in current time is related to modeling of the RSS as a random field (i.e. spatial map developing in time t) that satisfies some dynamical state equation. Following the typical linear assumptions for development of the RSS in time [8], [13], we represent its dynamical model in a vectorized space-time form defined via the following stochastic differential state equation of the first order

$$\frac{d\mathbf{z}(t)}{dt} = \mathbf{F}\mathbf{z}(t) + \mathbf{G}\boldsymbol{\xi}(t) \quad , \qquad \boldsymbol{\Lambda}(t) = \mathbf{C}\mathbf{z}(t) \qquad (20)$$

where $\mathbf{z}(t)$ is the so-called model *state vector*; $\mathbf{C}$ defines a linear operator that introduces the relation between the RSS $\boldsymbol{\Lambda}(t)$ and the state vector $\mathbf{z}(t)$, and $\boldsymbol{\xi}(t)$ represents the white model generation noise vector characterized by the statistics, $\langle\boldsymbol{\xi}(t)\rangle = \mathbf{0}$ and $\langle\boldsymbol{\xi}(t)\boldsymbol{\xi}^{T}(t')\rangle = \mathbf{P}_{\xi}(t)\delta(t-t')$ [8]. Here, $\mathbf{P}_{\boldsymbol{\xi}}(t)$ is referred to as state model disperse matrix [8] that characterizes the dynamics of the state variances developed in a continuous time t ($t_0 \to t$) starting from the initial instant t_0.

Next, the dynamic model equation that states the relation between the time-dependent SSP (actual scene image) $\mathbf{B}(t)$ and the desired RSS map $\boldsymbol{\Lambda}(t)$ can be represented as [8]

$$\hat{\mathbf{B}}(t) = \mathbf{L}\mathbf{C}\mathbf{z}(t) + \mathbf{v}(t) = \mathbf{H}(t)\mathbf{z}(t) + \mathbf{v}(t); \quad \mathbf{H}(t) = \mathbf{L}\mathbf{C}. \qquad (21)$$

Here, we introduced the linearized approximation $\mathbf{L}$ (i.e. first order matrix-form approximation [13] to the inverse of the RSS operator $\Lambda(\hat{B}(\mathbf{r}))$ and generalized (21) for the case of dynamical (i.e. time-dependent) RSS and SSP models. The stochastic differential model (20), (21) allows now to apply the theory of dynamical filters [8], [9], [13] to reconstruct the desired RRS in current time incorporating the a priori model dynamical information about the RSS. The aim of the dynamic filtration is to find an optimal estimate of the desired RSS, $\hat{\boldsymbol{\Lambda}}(t) = \mathbf{C}\hat{\mathbf{z}}(t)$, developed in current time, t ($t_0 \to t$), via processing the reconstructed image vector $\hat{\mathbf{B}}(t)$ (i.e. the reconstructed SSP developed in time) taking into considerations the a-priori dynamic model of the desired RSS specified through the state equation (20).

In other words, one have to design an optimal dynamic filter that when applied to the reconstructed image $\hat{\mathbf{B}}(t)$ (specified by the dynamic image model (21)) provides the optimal estimation of the desired RSS map

$\hat{\mathbf{\Lambda}}(t) = \mathbf{C}\hat{\mathbf{z}}(t)$, in which the state vector estimate $\hat{\mathbf{z}}(t)$ satisfies the a-priori dynamic behavior modeled by the stochastic dynamic state equation (20). The canonical discrete-time solution to (20) in *state variables* is [9], [13]

$$\begin{aligned} &\mathbf{z}(i+1) = \mathbf{\Phi}(i)\mathbf{z}(i) + \mathbf{\Gamma}(i)\mathbf{x}(i), \\ &\mathbf{\Lambda}(i) = \mathbf{C}\mathbf{z}(i) \end{aligned} \qquad (22)$$

where $\mathbf{\Phi}(i) = \mathbf{F}(t_i)\Delta t + \mathbf{I}$; $\mathbf{\Gamma}(i) = \mathbf{G}(t_i)\Delta t$, and Δt represents the time sampling interval for dynamical modeling of the RSS in discrete time. Next, we specify the statistical characteristics of the a-priori information in such a discrete time scale [8]. These are as follows:

- generating noise model

$$\{\boldsymbol{\xi}(i)\}: \langle \boldsymbol{\xi}(i) \rangle = \mathbf{0}; \ \langle \boldsymbol{\xi}(i)\boldsymbol{\xi}^T(j) \rangle = \mathbf{P}_{\xi}(i,j); \qquad (23)$$

- data noise

$$\{\mathbf{v}(i)\}: \langle \mathbf{v}(k) \rangle = \mathbf{0}; \ \langle \mathbf{v}(i)\mathbf{v}^T(j) \rangle = \mathbf{P}_{\mathbf{v}}(i,j); \qquad (24)$$

- state vector

$$\{\mathbf{z}(k)\}: \langle \mathbf{z}(0) \rangle = \mathbf{m}_z(0); \ \langle \mathbf{z}(0)\mathbf{z}^T(0) \rangle = \mathbf{P}_{\mathbf{z}}(0) \qquad (25)$$

where 0 argument implies the initial state for initial time instant, $i = 0$. For such model conventions, the disperse matrix $\mathbf{P}_z(0)$ satisfies the following *disperse* dynamic equation [13]

$$\begin{aligned} &\mathbf{P}_{\mathbf{z}}(i+1) = \langle \mathbf{z}(i+1)\mathbf{z}^T(i+1) \rangle \\ &= \mathbf{\Phi}(i)\mathbf{P}_{\mathbf{z}}(i)\mathbf{\Phi}^T(i) + \mathbf{\Gamma}(i)\mathbf{P}_{\xi}(i)\mathbf{\Gamma}^T(i). \end{aligned} \qquad (26)$$

6.2 Dynamic RSS reconstruction

The problem now is to design an optimal decision procedure (optimal filter) that, when applied to all reconstructed images $\{\hat{\mathbf{B}}(i)\}$ (ordered in a discrete time *i,* ($i_0 \to i$)), provides an optimal solution to the desired RSS $\mathbf{\Lambda}(i)$ represented via the estimate of the state vector state vector $\mathbf{z}(i)$ subject to the numerical dynamic model (19). To proceed with derivation of such a filter, we first represent the state equation (22) in discrete time *i,* ($i_0 \to i$):

$$\mathbf{z}(i+1) = \mathbf{\Phi}(i)\mathbf{z}(i) + \mathbf{\Gamma}(i)\boldsymbol{\xi}(i). \qquad (27)$$

Next, according to this dynamical model, the anticipated mean value for the state vector can be expressed as

$$\mathbf{m}_{\mathbf{z}}(i+1) = \langle \mathbf{z}(i+1) \rangle = \langle \mathbf{z}(i+1) | \hat{\mathbf{z}}(i) \rangle. \qquad (28)$$

The $\mathbf{m}_z(i+1)$ is considered as the a-priori conditional mean-value of the state vector for the $(i+1)$st estimation step, thus from (27), (28) we obtain

$$\begin{aligned} \mathbf{m}_z(i+1) &= \mathbf{\Phi}\langle \mathbf{z}(i) | \hat{\mathbf{B}}(0), \hat{\mathbf{B}}(1), ..., \hat{\mathbf{B}}(i) \rangle + \mathbf{\Gamma}\langle \boldsymbol{\xi}(i) \rangle \\ &= \mathbf{\Phi}\hat{\mathbf{z}}(i), \end{aligned} \qquad (29)$$

and the prognosis of the mean-value becomes, $\mathbf{m}_{\mathbf{z}}(i+1) = \mathbf{\Phi}\hat{\mathbf{z}}(i)$. From (27)…(29) one may deduce that given the fact that the particular reconstructed image $\hat{\mathbf{B}}(i)$ is treated at discrete time *i*, it makes the previous reconstructions $\{\hat{\mathbf{B}}(0), \hat{\mathbf{B}}(1), ..., \hat{\mathbf{B}}(i-1)\}$ irrelevant, hence the optimal filtering strategy is reduced to the dynamical one-step predictor.

Thus, using these derivations, we next modify the dynamical estimation strategy to such one-step optimal prediction procedure as follows,

$$\begin{aligned} \hat{\mathbf{z}}(i+1) &= \langle \mathbf{z}(i+1) | \hat{\mathbf{B}}(0), \hat{\mathbf{B}}(1), ..., \hat{\mathbf{B}}(i), \hat{\mathbf{B}}(i+1) \rangle \\ &= \langle \mathbf{z}(i+1) | \hat{\mathbf{z}}(i); \hat{\mathbf{B}}(i+1) \rangle = \langle \mathbf{z}(i+1) | \hat{\mathbf{B}}(i+1); \mathbf{m}_z(i+1) \rangle. \end{aligned} \qquad (30)$$

Hence, for the current $(i+1)$-st discrete-time prediction-estimation step, the dynamical RSS estimate (21) becomes

$$\hat{\mathbf{B}}(i+1) = \mathbf{H}(i+1)\mathbf{z}(i+1) + \mathbf{v}(i+1) \qquad (31)$$

with the a-priori predicted mean (28) for the desired state vector.

Applying now the Wiener minimum risk strategy [13] to solve (31) with respect to the state vector $\mathbf{z}(t)$ and taking into account the a priori information summarized by (23)…(25), the dynamic solution for the RSS state vector is

$$\begin{aligned} \hat{\mathbf{z}}(i+1) &= \mathbf{m}_z(i+1) + \\ &+ \mathbf{\Sigma}(i+1)\left[\hat{\mathbf{B}}(i+1) - \mathbf{H}(i+1)\mathbf{m}_z(i+1)\right] \end{aligned} \qquad (32)$$

where the desired dynamic filter operator $\mathbf{\Sigma}(i+1)$ is defined as follows,

$$\mathbf{\Sigma}(i+1) = \mathbf{K}_{\mathbf{\Sigma}}(i+1)\mathbf{H}^T(i+1)\mathbf{P}_{\mathbf{v}}^{-1}(i+1); \qquad (33)$$

$$\mathbf{K}_{\mathbf{\Sigma}}(i+1) = \left[\mathbf{\Psi}_{\mathbf{\Sigma}}(i+1) + \mathbf{P}_{\mathbf{z}}^{-1}(i+1)\right]^{-1}; \qquad (34)$$

$$\mathbf{\Psi}_{\mathbf{\Sigma}}(i+1) = \mathbf{H}^T(i+1)\mathbf{P}_{\mathbf{v}}^{-1}(i+1)\mathbf{H}(i+1). \qquad (35)$$

Last, using the derived filter equations (32), (35) and the initial RSS state model given by (22), we finally obtain the optimal filtering procedure for dynamic reconstruction of the desired RSS map in the current discrete time

$$\begin{aligned} \hat{\mathbf{\Lambda}}(i+1) &= \mathbf{\Phi}(i)\hat{\mathbf{z}}(i) + \\ &+ \mathbf{\Sigma}(i+1)\left[\hat{\mathbf{B}}(i+1) - \mathbf{H}(i+1)\mathbf{\Phi}(i)\hat{\mathbf{z}}(i)\right]; \\ &i = 0, 1, \ldots \end{aligned} \qquad (36)$$

with the initial condition, $\hat{\mathbf{\Lambda}}(0) = \Lambda\{\hat{\mathbf{B}}(0)\}$, and a priori statistics specified by (23)…(25).

Figure 1 shows the information flow diagram that illustrates the overall fused procedure for RSS reconstruction and dynamic filtration. As a primary part, the SSP image reconstruction is to be performed. Next, the desired particular RSS map is to be reconstructed in a dynamic fashion.

The crucial issue to note here is related to model uncertainties regarding the particular employed dynamical RSS model (22), hence the corresponding uncertainties regarding the overall dynamically reconstructed RSS.

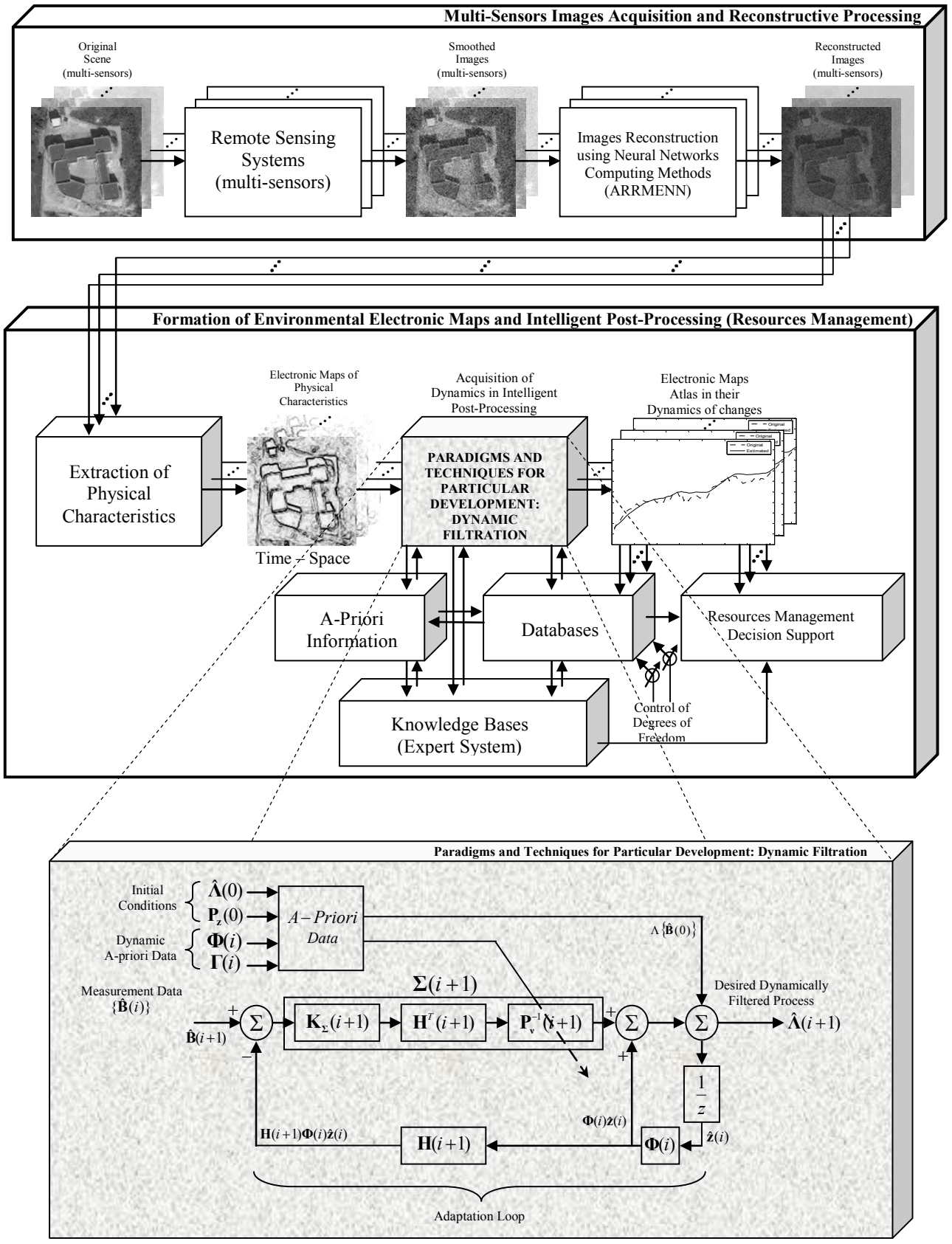

Fig. 1. Block diagrams of the image and RSS reconstruction and dynamical post-processing techniques.

SNR, μ	FIRST SYSTEM, $\Delta\Psi_a = 16$		SECOND SYSTEM, $\Delta\Psi_a = 32$	
[dB]	$IOSNR^{(RSF)}$ [dB]	$IOSNR^{(ASF)}$ [dB]	$IOSNR^{(RSF)}$ [dB]	$IOSNR^{(ASF)}$ [dB]
15	2.24	3.20	2.62	3.89
20	3.34	4.32	4.47	5.78
25	4.20	5.12	5.31	7.42
30	5.55	6.24	6.45	9.19

Table 1. IOSNR Values

7. QUALITY METRIC

For the purpose of objectively testing the performances of different FBR-related SSP estimation algorithms, a quantitative evaluation of the improvement in the estimates (gained due to applying the suboptimal and optimal IFOs $\mathbf{F}^{(RSF)}$ and $\mathbf{F}^{(ASF)}$ (instead of the adjoint operator $\mathbf{F}^{(MSF)} = \mathbf{S}^{+}$) was accomplished. In analogy to image reconstruction [5] we use the quality metric defined as an improvement in the output signal-to-noise ratio [9]

$$IOSNR^{(RSF/ASF)} = 10\log_{10}\frac{\sum_{k=1}^{K}\left(\hat{B}_k^{(MF)} - B_k\right)^2}{\sum_{k=1}^{K}\left(\hat{B}_k^{(RSF/ASF)} - B_k\right)^2} \quad (37)$$

8. COMPUTER SIMULATIONS

In the simulations, we investigated the performances of the family of all the FBR-based methods summarized above in their applications to reconstructive RS imagery. We simulated conventional side-looking imaging radar (i.e. the radar array was constructed by the moving antenna as in [6]) with the SFO factored along two axes in the imaging plain. In the range direction (over the vertical axis), the radar ambiguity function was approximated by a triangular shape pulse [3] of three pixels width at a half-maximum level and in the azimuth direction (over the horizontal axis) the ambiguity function was approximated by a Gaussian bell of 8 pixels width [6], [13]. Figure 2 presents the initial image of the reported here scene formed applying the *MSF* method, i.e. $\hat{\mathbf{B}}_{MSF}$, contaminated with 8% additive white noise. All other images correspond to different reconstructive FBR-based methods as specified in the corresponding figure captions.

The Table 1 shows the IOSNR values provided with two of the simulated methods: RSF and ASF, i.e. FBR-MVDR. The results are reported for two SAR system models with different resolution parameters and different SNR.

Next, in Figures 8.a, 8.c and 8.e, we present some simulation results of dynamic reconstruction-filtration of a particular RSS that represents the so-called *integral hydrological index* (IHI) map extracted from the reconstructed images [9]. The particular reported simulations are specified in the figure captions. The IHI map is extracted from the original brightness reconstructed image applying the truncated (two-edge) histogram filter operator with the empirically adjusted lower threshold th_L and upper threshold th_U [9]. Within the truncation interval ($th_U - th_L$), the IHI extraction operator provides homogeneous translation of the scaled reconstructed images $\{\hat{\mathbf{B}}\}$ in to the RSS map $\{\mathbf{\Lambda}\}$ [9], [13]. Also, in Figures 8.b, 8.d and 8.f, we present the simulation results of the dynamic behavior of the IHI maps extracted/filtered from the ASF-reconstructed SSP image, RSF and FBR-MVDR reconstructed images, respectively. The reported filtered IHIs are indicative of the dynamical behavior of the RSS. The IHI map dynamics are well detailed in both reported simulation experiments. Also, the dynamical reconstructions performed iteratively applying the algorithm (36) resulted in the processing with substantial reduced computational load. The reported results qualitatively demonstrate that with proper adjustment of the degrees of freedom in the general algorithm (36), one could predict the dynamic behavior of the IHI maps. The detailed investigation of the prediction methodology is a matter of the further studies.

9. DISCUSSIONS AND CONCLUSION

In this study, we addressed the new fused Bayesian-regularization (FBR) paradigm for estimating the SSP that combines the Bayesian inference strategy with the descriptive regularization techniques. With this method, we presented the FBR-based interpretation of the conventional matched spatial filtering and new recently developed RSF and ASF techniques that manifest the enhanced resolution performances of the remotely sensed environmental images. Also, we examined the behaviour and performances of a family of the recently developed FBR-based SSP estimators in application to the reconstructive RS imagery. The advantages of the well designed RI experiments (that employ the FBR, ASF and FBR-MVDR algorithms) over the cases of poorer designed experiments (that employ the MSF, CLS and WCLS methods) were investigated and reported here for one test scene borrowed from the real-world RS imagery.

These results qualitatively demonstrate that with some proper adjustment of the degrees of freedom of the robustified FBR-based techniques (i.e. the RFBR, ASF and FBR-MVDR), one could approach the quality of the statistically optimal general FBR method avoiding the cumbersome adaptive computations. The resolution is substantially improved for the cases when any of three techniques (RFBR, ASF and FBR-MVDR) was applied to enhance the RS images, i.e. regions of interest are much better defined, and ringing effects are within the acceptable tolerance level. The iterative RFBR and the FBR-MVDR techniques somewhat overperform the ASF algorithm but require almost 10 times more computations than the ASF algorithm.

Fig. 2. Rough Image formed applying the matched spatial filtering (MSF) technique.

Fig. 5. Enhanced radar image formed applying the adaptive spatial filtering (ASF) algorithm.

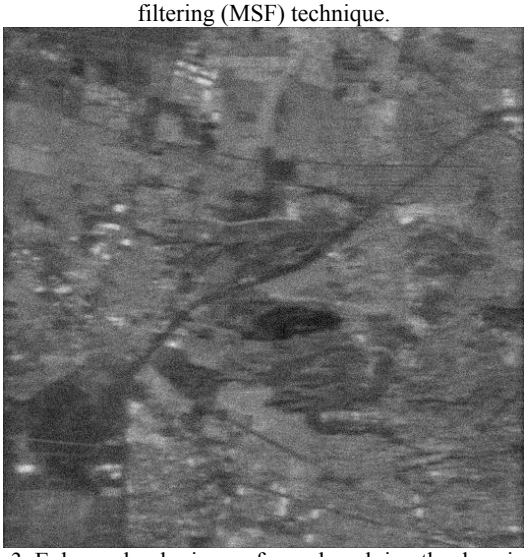

Fig. 3. Enhanced radar image formed applying the descriptive constrained least squares (CLS) algorithm.

Fig. 6. Enhances radar image formed applying the robust FBR estimator.

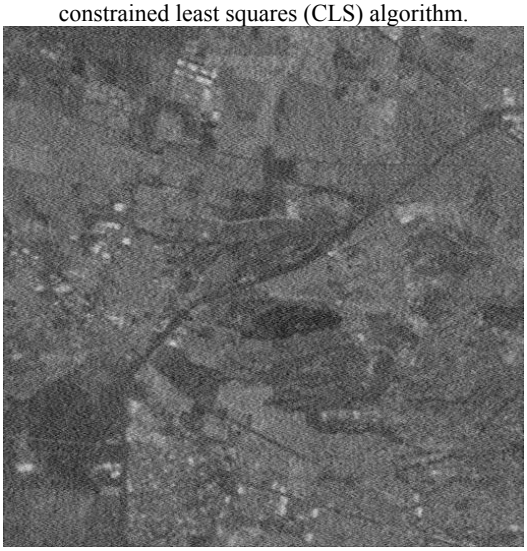

Fig. 4. Enhanced radar image formed applying the modified descriptive weighted constrained least squares (WCLS).

Fig. 7. Enhances radar image formed using the aggregated FBR-MVDR algorithm.

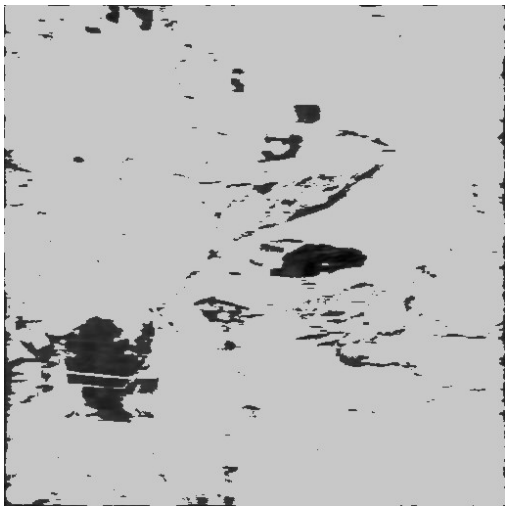

(a) Integral Hydrological Index (IHI) map extracted from the reconstructed figure 5

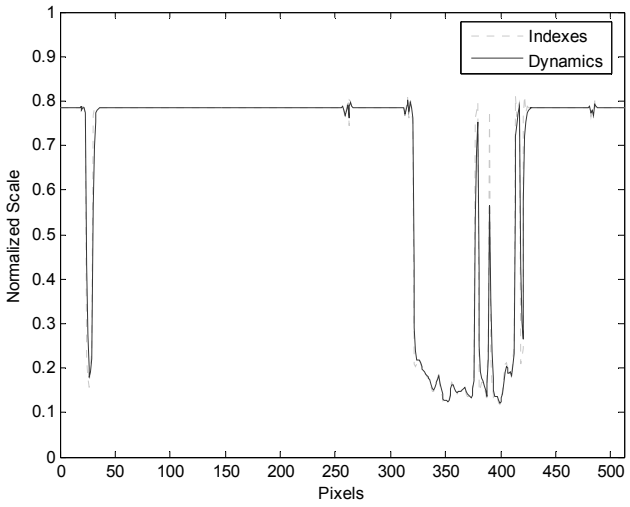

(b) Dynamics for a particular zone of the IHI map extracted from figure 8(a)

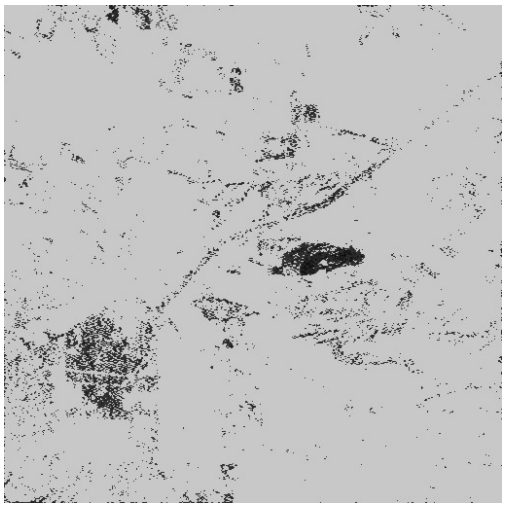

(c) Integral Hydrological Index (IHI) map extracted from the reconstructed figure 6

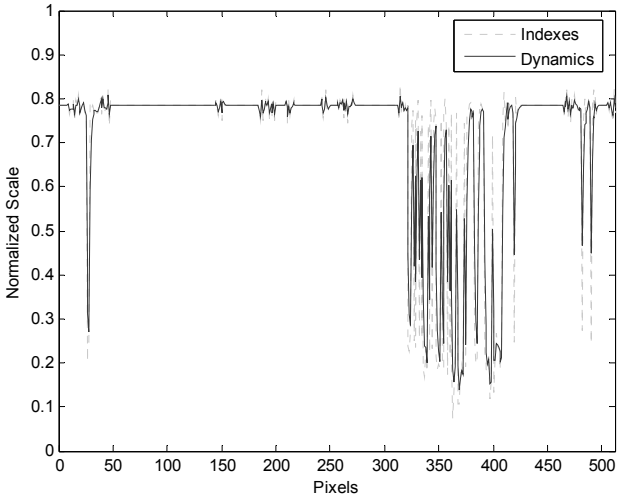

(d) Dynamics for the same particular zone of the IHI map extracted from figure 8(c)

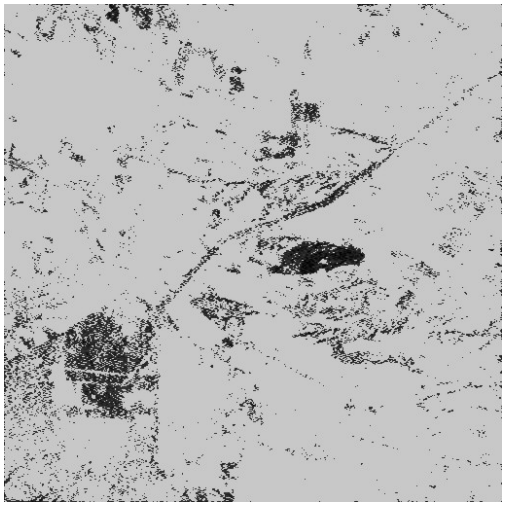

(e) Integral Hydrological Index (IHI) map extracted from the reconstructed figure 7

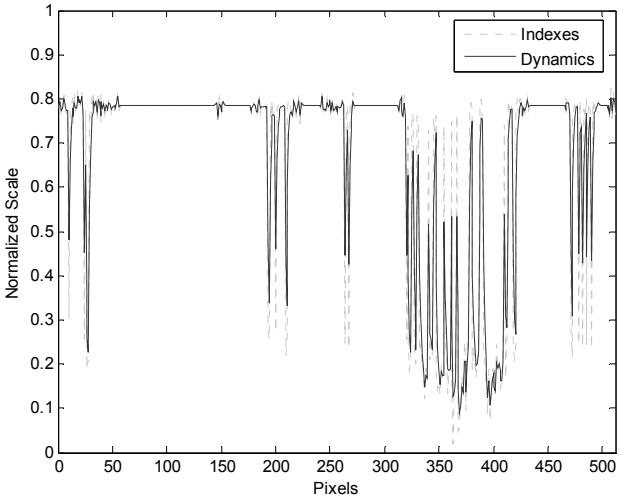

(f) Dynamics for the same particular zone of the IHI map extracted from figure 8(e)

Fig. 8. Simulation results of post-processing and dynamical filtration of the RSS using SAR data

The optimization of the adjustments of the regularization degrees of freedom could further enhance the performances of all three reported methods and reduce the computational load. Such optimization is a matter of the further studies.
Also, as a matter for perspective study, we have addressed the dynamical RSS post-processing scheme that reveals some possible approach toward a new dynamic computational paradigm for high-resolution fused numerical reconstruction and filtration of different RSS maps in current time. In future work, we intend to develop a family of such dynamical versions of the FBR-based algorithms for updating the relevant RSS maps in current discrete time.

References

[1] Synthetic Aperture Radar, L.G. Cutrona, 2nd ed., M.I. Skolnik, Ed. In chief, MA: McGraw Hill, 1990.

[2] Adaptive Radar Detection & Estimation, S. Haykin and A. Steinhardt, New York: Wiley, 1992.

[3] Principles and Applications of Imaging Radar, Manual of Remote Sensing, F.M. Henderson and A. V. Lewis, 3rd ed. New York, 1998, vol. 3.

[4] Estimation of Wavefield Power Distribution in the Remotely Sensed Environment: Bayesian Maximum Entropy Approach, Y.V. Shkvarko, IEEE Transactions on Signal Processing, vol. 50, pp. 2333-2346, September 2002.

[5] Unifying Regularization and Bayesian Estimation Methods for Enhanced Imaging with Remotely Sensed Data. Part I – Theory, Y.V. Shkvarko, IEEE Transactions on Geoscience and Remote Sensing, pp. 923-931, March 2004.

[6] Unifying Regularization and Bayesian Estimation Methods for Enhanced Imaging with Remotely Sensed Data. Part II – Implementation and Performance Issues, Y.V. Shkvarko, IEEE Transactions on Geoscience and Remote Sensing, vol. 42, pp. 932-940, March 2004.

[7] Theoretical Aspects of Array Radar Imaging via Fusing Experiment Design and Descriptive Regularization Techniques, Y.V. Shkvarko, 2nd IEEE Sensor Array and Multichannel Signal Processing Workshop, Washington D.C. U.S.A., August 2002.

[8] Optimal Reception of Space-Time Signals in Radio Channels With Scattering, S.E. Falkovich, V.I. Ponomaryov, and Y.V. Shkvarko, Moscow: Radio I Sviaz Press, 1989.

[9] Computational Enhancement of Large Scale Environmental Imagery: Aggregation of Robust Numerical Regularization, Neural Computing and Digital Dynamic Filtering, Y.V. Shkvarko and I.E. Villalon-Turrubiates, International Journal of Computational Science and Engineering (IJCSE), Interscience Publishers, U.S.A., 2006.

[10] Simulation Study of the Unified Bayesian-Regularization Technique for Enhanced Radar Imaging, Y.V. Shkvarko and I.E. Villalon-Turrubiates, 2nd International Radio Electronic Forum (IREF), Kharkov Ukraine, September 2005.

[11] Unified Bayesian-Experiment Design Regularization Technique for High-Resolution of the Remote Sensing Imagery, Y.V. Shkvarko and Ivan E. Villalon-Turrubiates, 1st IEEE International Workshop on Computational Advances in Multi-Sensor adaptive processing (CAMSAP), Puerto-Vallarta Mexico, December 2005.

[12] Cognitive Reconstructive Remote Sensing for Decision Support in Environmental Resource Management, I.E. Villalon-Turrubiates and Y.V. Shkvarko, 17th Information Resources Management Association (IRMA) International Conference, Washington D.C. U.S.A., May 2006.

[13] Intelligent Processing for SAR Imagery for Environmental Management, I.E. Villalon-Turrubiates, 17th Information Resources Management Association (IRMA) International Conference, Washington D.C. U.S.A., May 2006.